Modeling Glutaric Aciduria Type I in human neuroblastoma cells recapitulates neuronal damage that can be rescued by gene replacement

Mateu-Bosch A[1#], Segur-Bailach E [1,2#], García-Villoria J[1,2,3,4], Gea-Sorlí S[1,2], Ruiz I[5], del Rey J[5], Camps, J[1,5,6], Guitart-Mampel M[1,2],[4,7], Garrabou G[1,2,4,7], Tort F[1,2,4], Ribes A[1,2,4], Fillat C[1,2,7]

[1]Institut d'Investigacions Biomèdiques August Pi i Sunyer (IDIBAPS), Barcelona, Spain

[2]Centro de Investigación Biomédica en Red de Enfermedades Raras (CIBERER), Barcelona,Spain

[3]Section of Inborn Errors of Metabolism-IBC, Biochemial and Molecular Genetics Department, Hospital Clinic de Barcelona, Barcelona, Spain

[4]Inherited Metabolic Diseases and Muscle disorders' Research Group

[5]Unitat de Biologia Cel·lular i Genètica Mèdica, Departament de Biologia Cel·lular, Fisiologia i Immunologia, Facultat de Medicina, Universitat Autònoma de Barcelona, Bellaterra, 08193, Spain

[6]Centro de Investigación Biomédica en Red de Enfermedades Hepáticas y Digestivas (CIBEREHD), Barcelona, Spain

[7]Facultat de Medicina i Ciències de la Salut. Universitat de Barcelona (UB), Barcelona, Spain

# Equal contribution

* Corresponding author: Cristina Fillat, E-mail:cfillat@recerca.clinic.cat. Institut d'Investigacions Biomèdiques August Pi i Sunyer (IDIBAPS), 08036 Barcelona, Spain

ABSTRACT

Glutaric Aciduria type I (GA1) is a rare neurometabolic disorder caused by mutations in the *GDCH* gene encoding for glutaryl-CoA dehydrogenase (GCDH) in the catabolic pathway of lysine, hydroxylysine and tryptophan. GCDH deficiency leads to increased concentrations of glutaric acid (GA) and 3-hydroxyglutaric acid (3-OHGA) in body fluids and tissues. These metabolites are the main triggers of brain damage. Mechanistic studies supporting neurotoxicity in mouse models have been conducted. However, the different vulnerability to some stressors between mouse and human brain cells reveals the need to have a reliable human neuronal model to study GA1 pathogenesis.

In the present work we generated a *GCDH* knockout (KO) in the human neuroblastoma cell line SH-SY5Y by CRISPR/Cas9 technology. SH-SY5Y-*GCDH* KO cells accumulate GA, 3-OHGA, and glutarylcarnitine when exposed to lysine overload. GA or lysine treatment triggered neuronal damage in GCDH deficient cells. SH-SY5Y-*GCDH* KO cells also displayed features of GA1 pathogenesis such as increased oxidative stress vulnerability. Restoration of the GCDH activity by gene replacement rescued neuronal alterations. Thus, our findings provide a human neuronal cellular model of GA1 to study this disease and show the potential of gene therapy to rescue GCDH deficiency.

INTRODUCTION

Glutaric aciduria type I (GA1, OMIM #231670) is an autosomal recessive disorder of lysine (Lys), hydroxylysine and tryptophan catabolism, due to the deficiency of glutaryl-CoA dehydrogenase (GCDH, EC 1.3.99.7). GCDH is a homotetrameric mitochondrial flavin adenine dinucleotide (FAD)-dependent enzyme, that catalyzes the oxidative decarboxylation of glutaryl-CoA to crotonyl-CoA and CO_2. Mutations in this gene cause a deficiency of GCDH that leads to the accumulation of glutaric (GA) and 3-hydroxyglutaric (3-OHGA) acids, as well as glutarylcarnitine (C5DC) and to a depletion of carnitine in tissues and body fluids. It was described for the first time in 1975 by Goodman and colleagues (1). Since then, more than 200 mutations have been reported in the Human Gene Mutation Database (HGMD; www.hgmd.cf.ac.uk) and have been recently reviewed in Schuurmans et al 2023 (2).Genotype-phenotype correlation has not always been verified, but interestingly, an in silico model has recently shown to predict high pathogenicity in the genotypes causing low enzyme activity (3). The estimated prevalence of the disease is about 1:100,000 in Caucasians. Clinically, GCDH deficiency is characterized by acute degeneration of the caudate and putamen, severe dystonic-dyskinetic disorder, hypotonia and irritability that generally occurs between 3 and 36 months of age during encephalopathic crises precipitated by febrile illnesses, surgical processes or even routine vaccinations (4–9), but a relevant number of patients have symptoms such as macrocephaly and delayed motor development during the first weeks of life. The majority (90-95%) of untreated individuals develop irreversible striatal damage and, subsequently, a complex movement disorder with predominant dystonia (5,10).

GA1 knockout (KO) mouse model with complete loss of GCDH (*Gcdh*−/−) presents similar biochemical abnormalities to those found in patients (11). However, these KO mice did not

show relevant neurologic symptoms unless they were fed with high Lys diet (11–13). Elevated levels of GA and 3-OHGA in the brain have been proposed as the main triggers of neuronal toxicity(14,15). Excitotoxicity, disruption of energy metabolism and redox homeostasis, oxidative stress, and alteration of the glutamatergic and GABAergic systems, as well as blood–brain barrier breakdown in the cerebral cortex and striatum of *Gcdh*−/− mice exposed to a high protein or Lys diet have been proposed as pathogenic processes (9,12,13,15). However, the cellular mechanisms leading to neuronal damage in GA1 remains unclear. Until now most of the studies have been conducted in tissues and cells derived from mouse or rat models but a human neuronal model to interrogate GA1 condition is lacking. The SH-SY5Y cells are human neuroblastoma cells, which are comparable to neurons with regards to their morphological, neurochemical and electrophysiological properties and have been extensively used to evaluate neuronal injury or mitochondrial dysfunction in brain pathology (14,16).

In the present work we generated and characterized an SH-SY5Y human neuronal cell model of GCDH deficiency by using CRISPR-Cas9 technology to develop *GCDH* KO cells. We also explored the potential of restoring GCDH defects through gene replacement. We observed that high Lys exposure of *GCDH* KO cells resulted in the accumulation of neurotoxic metabolites and triggered alterations in the mitochondrial redox homeostasis, recapitulating the disease phenotype. Delivery of the *GCDH* cDNA under the human 3-phosphogycerate kinase (PGK) promoter restored GCDH activity and prevented from the cellular damage. In addition, the generated model could be appropriate to perform molecular studies to improve understanding of the physiopathology of the disease as well as to test potential therapies for GA1.

MATERIALS AND METHODS

Plasmids

pLentiCRISPRv2_*GCDH*: CRISPR guides that target *GCDH* were selected using the CRISPR guide selection software from Feng Zhang's laboratory (https://zlab.bio/guide-design-resources). Guides (sgRNA1: CTCGCTCTGAGAGAGCATGG; sgRNA2: CGGGAGAACACAGAGCCAAC; sgRNA3: CCAGTCAAACTCGGGACGCG) targeting exons 3 and 4 of the *GCDH* gene were cloned into the pLentiCRISPR v2 plasmid (Addgene #52961, Watertown, MA, USA) containing hSpCas9 and puromycin genes, following manufacturer's protocol. For gene editing experiments, we used plasmids: pLentiCRISPR v2 (Addgene #52961) and the dsDNA donor. Oligos were annealed and subsequently cloned into the pLentiCRISPR v2 plasmid, followed by Sanger sequencing, according to manufacturer's protocol.

pEGFP/PGK-*GCDH*: The construct was generated using elements from the pCCL.PGK.*FANCA*.WPRE backbone (17). This plasmid contains the EGFP gene that will be expressed upon integration allowing for the FACSorting of gene-targeted cells. The FANCA gene from the pCCL.PGK.*FANCA* plasmid was removed and substituted by the *GCDH* gene (p*GCDH* from PlasmID Repository, Boston, MA, USA) to generate pEGFP/PGK-*GCDH*. In this construct the *GCDH* gene is under the transcriptional control of the human PGK promoter.

Cell lines and cellular models

The human neuroblastoma cell line SH-SY5Y was obtained from American Type Culture Collection (ATCC, Manassas, VA, USA) and cultured in DMEM/F12 medium supplemented with fetal bovine serum (FBS), penicillin (100 µg/mL), and streptomycin (100 µg/mL) (Gibco-BRL, Carlsbad, CA, USA), and maintained in a humidified atmosphere of 5% CO2 at 37°C.

Differentiation of neuroblastoma SH-SY5Y cells to neuronal cultures was performed on an 18 days period in the presence of retinoic acid and brain-derived neurotrophic factor (BDNF) following the protocol described by Shipley and collaborators (18).

SH-SY5Y-*GCDH*-KO cells were generated by CRISPR/Cas9 technology. pLentiCRISPRv2_*GCDH* was electroporated into SH-SY5Y cells with the Neon® Transfection System MPK5000 (Invitrogen, Carlsbad, CA, USA). Electroporation conditions followed voltage, pulse and time parameters suggested by the Neon website for SH-SY5Y. Cells were exposed to 2 weeks of puromycin selection (2.5 μg/ml) and plated as single cells. Individual clones were tested by western blot for loss of GCDH expression and genetic alterations at the *GCDH* gene were confirmed by Sanger sequencing.

SH-SY5Y-*GCDH*-GI cells were generated by nucleofection. For this, the SH-SY5Y-*GCDH*-KO1 clone cells were nucleofected by Neon® Transfection System MPK5000 (Invitrogen) with the pEGFP/PGK-*GCDH* cassette. One week later, cells expressing EGFP were selected by FACSorting in a FACSCanto II (Becton Dickinson, Franklin Lakes, NJ, USA) and expanded. The expression of GCDH was tested by western blot.

Cell counting assay

Hoechst 33342 (H3570, Invitrogen) was added to cells at a final concentration of 1 μg/mL for 30 min at 37°C. Fluorescence intensity was measured in a plate reader (Tecan M200 Pro, Männedorf, Switzerland). Excitation and emission wavelengths were 361nm and 486nm.

Apoptosis detection by flow cytometry

Apoptosis was quantified by double-staining with annexin V conjugated to fluorescein isothiocyanate and propidium iodide (88-8005-74, Invitrogen). Ten thousand cells per sample were acquired in BD FACS CANTOTM II and the proportions of labeled cells were analyzed using FlowJo v10 Software (Asland, OR, USA).

Blue native polyacrylamide gel electrophoresis (BN-PAGE)

Cell pellets were resuspended in Mannitol buffer (225mM Mannitol, 75mM Sucrose, 10mM Tris-HCl and 0.1mM EDTA) and Dounce homogenized (20 strokes) on ice. Cell debris and nuclei were removed by centrifugation twice at 650g for 20 min at 4 °C. After determining the protein concentration with a BCA assay, mitochondria-enriched pellets were obtained from the volume equivalent to 600ug of protein, as described -previously (19). Samples were loaded in a 4% to 20% polyacrylamide gradient gels and electrophoresed in non-denaturing conditions. GCDH in gel activity was performed by incubating the gel in an activity buffer (50mM Phosphate buffer, 200 µM Glutaryl CoA, 1,5 µM FAD and 2mg/ml NBT) at 37 °C O/N.

Metabolite analysis

Cell extracts were obtained as described above. Then, protein precipitation and C5DC extraction were perform with organic solvent containing C5DC-d5 used as internal standard (NeoBase 1 kit, Perkin Elmer, Waltham, MA, USA). After centrifugation, the supernatant was dried under nitrogen and derivatized with n-butanol/HCl 3N, dried again, and finally reconstituted in methanol/H2O (75/25). The analysis was performed in a ACQUITY UPLC systemI-Class- XevoTQD tandem mass spectrometry (Waters, Beverly, MA,USA) by direct infusion using electrospray positive ionization and MRM mode (Masslynx software 4.1,

Waters). The mobile phase used was the one included in Neobase 1 kit. The quantifications were performed in Neolynx software, (Waters).

For GA and 3-OHGA analysis, an aqueous solution containing deuterium labeled internal standards GA-d4 and 3-OH-GA-d5 were added to cell extracts and were subjected to an Oasis HLB 96-well Plate (30mg sorbent) extraction system. These metabolites were then eluted by acetonitrile/methanol (90/10) phase. To facilitate ionization formic acid at 0,4% solution was added. The analysis was done on an ACQUITY UPLC system H-Class-Xevo TQS tandem mass spectrometry (Waters). The chromatographic separation was performed on an ACQUITY Premier BEH C18 Column (1.7 µm, 2.1 x 100 mm) at a flow rate of 310µL min–1 using an isocratic binary mixture of 95 % solvent A (water with 0.4% formic acid) and 5%solvent B (methanol with 0.4% formic acid). Detection was performed in electrospray positive and MRM mode (Masslynx software 4.1, Waters). Quantification was performed using a calibration curve (Targetlynx software, Waters) and normalized for protein content.

Mitochondrial Superoxide Levels analysis

Mitochondrial superoxide levels were measured by MitoSOXRed probe (M36008, Invitrogen). Experiments were performed following manufacturer's indications, incubating cells with 5 µM MitoSOXRed for 10 min at 37°C. Cells were trypsinised and resuspended in PBS. Fluorescence intensity was analyzed by flow cytometry (BD FACS CANTOTM II) and FlowJo v10 Software.

Thiobarbituric acid-reactive substances (TBARS)

Malondialdehyde (MDA) levels were measured by the method of thiobarbituric acid-reactive substances (TBARS) according to Janero DR(20). Briefly, 250 µL of cell homogenate, 250 µL of trichloroacetic acid (40%) and 250 µL of thiobarbituric were added in a 5ml glass tube. The mixture was incubated at 100 °C for 15 min. A calibration curve was performed using

1,1,3,3-tetramethoxypropane subjected to the same treatment as that of the samples. The reaction develops in a pink color that is proportional to the concentration of TBARS. The results were expressed as pmol TBARS/mg protein.

Statistical Analysis

Results were expressed as mean ± SEM of at least three independent experiments. Statistical differences were determined using Prism (GraphPad V8 software, San Diego, CA, USA). Unless otherwise stated differences between experimental groups were analyzed by the non-parametric Mann-Whitney U test. The level of significance was considered for P values < 0.05.

RESULTS AND DISCUSSION

Generation of the human neuroblastoma SH-SY 5Y *GCDH* KO model

A neuronal model of GA1 was generated by knocking out *GCDH* in SH-SY5Y cells using CRISPR/Cas9. We designed 3 different gRNAs (sgRNA1, sgRNA2 and sgRNA3) targeting *GCDH* exons 3 and 4. Guides fulfilled the criteria of binding to target sites 5' to the PAM sequence with minimal off target cross-reactivity. Selected guides were cloned into the pLentiCRISPRv2 plasmid that contains the Cas9 and a pool of the three guides were transfected into SH-SY5Y neuroblastoma cells and submitted to puromycin selection. Individual clones were analyzed for both genomic alterations and GCDH expression. The absence of GCDH protein confirmed the generation of three *GCDH* KO cell lines (Supplementary Fig. 1A). Clone 1 was selected for further studies and named as SH-SY5Y *GCDH*-KO.

GCDH insertion in *GCDH* KO cells restores GCDH activity.

To study whether *GCDH* gene transfer in the context of neuronal *GCDH* deficient cells could restore the enzyme deficiency and the associated cellular alterations, the SH-SY5Y *GCDH*-KO cells were modified with a vector expressing the *GCDH* gene to generate SH-SY5Y *GCDH*-GI cells. In this cassette the *GCDH* gene was under the transcriptional control of the human PGK (hPGK) promoter and the EGFP promoterless was expressed from a genomic promoter after integration.

SH-SY5Y *GCDH*-KO cells were transfected with the pEGFP/PGK-*GCDH* vector. EGFP expressing cells were FACS sorted and analyzed for genomic integration (Supplementary Fig. 1B). FISH analysis identified insertion of the transgene in the chromosome 19, in the *GCDH* region and in a non-targeted region (Supplementary Fig. 1C).

Genetic Insertion of the pEGFP/PGK-*GCDH* cassette in *GCDH* neuroblastoma KO cells generated the SH-SY5Y *GCDH*-GI cell line and resulted in the expression of the GCDH protein (Fig. 1A). The newly expressed protein displayed enzyme activity as shown by the in-gel activity assay performed by BN-PAGE (Fig. 1B).

Neuronal *GCDH*-KO cells recapitulate GA-I cellular alterations that are rescued in the gene-corrected cells.

To validate SH-SY5Y *GCDH*-KO cells as a human neuronal model to study GA1, we analyzed several parameters that have been associated to the neuropathology of this disease. GCDH deficiency in GA1 patients results in the accumulation of GA, 3-OHGA and C5DC in patient groups classified as high and low excretors (21). To evaluate whether *GCDH* neuroblastoma KO cells, were able to accumulate GA1 metabolites, cells were cultured with Lys 10mM, a dose considered to mimic the situation of a catabolic stress, to stimulate the Lys catabolic pathway (22,23). This supplementation led to a significant increase of the three metabolites, GA, 3-OHGA and C5DC in KO cells whereas the *GCDH*-GI model showed similar levels to WT cells (Fig. 1C). Thus, despite there is only a 50% protein rescue in the *GCDH*-GI model compared to WT cells, such GCDH activity would be sufficient to prevent metabolites increase.

The accumulation of GA and 3-OHGA in brain tissue are the main triggers of cellular damage in CNS cell types (15,16). However, neuronal susceptibility to cell death triggered by GA1 metabolites has been controversial with different vulnerabilities in mouse and rat neuronal cultures. Rat striatal neurons deficient in *GCDH* by lentivirus knockdown were found to undergo apoptosis (23,24). However, a very mild or even lack of induced toxicity has been observed after GA or Lys stimulation of striatal, hippocampal or cortical neurons of *Gcdh* -/- mice. Of notice, striatal neurons were vulnerable to GA or Lys stimulated astrocytes, suggesting an astrocyte contribution to the detrimental effects observed on primary neurons

(25). Such different response to GA1 metabolites induction of neuronal death might be related to particular inter-species vulnerabilities. In fact, genetic determinants of susceptibility to neuronal cell death have already been defined between certain strains of mice (26). Differences in response to cellular stress under identical insults have also been found between human and mouse neurons (27). Moreover, human astrocytes have been shown to exhibit greater susceptibility to oxidative stress than mouse astrocytes (28). Recently, a cross-species analysis of single-cell RNA seq highlighted expanded diversity between specific neurons of mice, non-human primates and humans (29). All these data, highlights the need to study neuronal response to GA1 metabolites not only in animal models but importantly in human neuronal models of GA1. In this line, we investigated the susceptibility of the human neuroblastoma SH-SY5Y *GCDH*-KO cells to GA or Lys overload. Exposure to GA triggered cellular toxicity in a dose-dependent manner (Fig. 2A). Such cellular mortality could probably be mediated by apoptosis since transcript levels of caspase-3 were increased (Fig. 2B), in line with previous work (24). Interestingly, these effects were not observed in cells reconstituted with GCDH function, demonstrating the specificity of the effects.

To determine whether Lys exposure compromises neuronal cell viability in *GCDH* deficient cells, SH-SY5Y WT, *GCDH*-KO and *GCDH*-GI were treated with 10 mM and 25 mM Lys for 24h. Exposure to Lys led to 30% and 50% decrease in the metabolic activity of the cells in the *GCDH*-KO but not in *GCDH*-GI (Fig. 3A). Similar results were observed in terminally differentiated neurons (Supplementary Fig. 2). In a Hoechst 33342 fluorometric assay Lys treatment revealed reduced fluorescent intensity in *GCDH*-KO but not in *GCDH*-GI cells neither in WT cells (Fig. 3B). Such effects were not associated to the activation of cell death by apoptosis since the number of apoptotic cells in *GCDH*-KO was not altered by the incubation with Lys in the Annexin V assay (Fig. 3C) neither by analysis of caspase-3 mRNA content (data not shown). It can be speculated that the amount of GA accumulated upon

10mM or 25mM Lys was not sufficient to activate an apoptotic program, at least after 24h exposure. However, these results suggest that high Lys triggered neuronal injury in *GCDH*-KO cells resulting in decreased metabolic activity and cell proliferation, that could be rescued by restoring GCDH activity. A proposed mechanism of neurotoxicity induced by GA and 3-OHGA metabolites is through the activation of oxidative stress. Menadione, a precursor in the synthesis of Vitamin K, is a potent inductor of ROS production and through an oxidative stress mechanism triggers cell death (30). Primary astrocytes from *Gcdh* -/- mice have shown increased vulnerability to menadione-induced oxidative stress (31). In this context, we studied the susceptibility of neuroblastoma *GCDH*-KO cells to menadione treatment. Incubation of menadione for 6h at 2.5μM and 3.5μM showed a dose-dependent decreased viability in the MTT assay that was not observed in SH-SY5Y *GCDH*-GI nor in WT cells, suggesting that *GCDH* KO cells were more susceptible to oxidative stress (Supplementary Fig. 3). Next, we investigated the induction of mitochondrial ROS upon Lys overload. A tendency to increased MitoSOXRed intensity was observed in all the cell lines (Fig. 4A). Interestingly, 10 mM Lys significantly augmented SOD concentration in *GCDH*-KO cells but not in the other cell lines, showing the activation of an antioxidant response in *GCDH*-KO cells, probably as a compensatory mechanism (Fig. 4B). We studied lipid peroxidation in these models since it is a well-known process where ROS attack lipids in cellular membranes generating toxic aldehydes like malondialdehyde (MDA) and 4-hydpdynonenal 4-HNE (32). Moreover, exposure of *Gcdh*-/- astrocytes to 10mM lysine has shown increased MDA levels and feeding *Gcdh*-/- mice with high Lys diet showed increased MDA in cortex and striatum (25,33). In line with these data where MDA content was increased in GCDH deficient cells exposed to high Lys, we observed that Lys treatment to neuroblastoma *GCDH*-KO cells triggered a significant increase in MDA that was not observed in gene-corrected SH-SY5Y *GCDH*-GI cells neither in WT cells (Fig. 4C). These results show higher vulnerability of the SH-SY5Y *GCDH*-KO to oxidative stress. Probably, a small increase in

reactive species may signal to activate antioxidant defenses, but deficient-GCDH cells could not successfully resolve making lipids vulnerable to oxidative damage. We can speculate that the neuronal damage detected in the human SH-SY5Y *GCDH*-KO model may possible reflect some of the abnormalities observed in affected patients.

In conclusion, the present results provide experimental evidence that neuroblastoma SH-SY5Y *GCDH*-KO can be a good human model to gain further insight into the neuronal defects of GCDH deficiency. Moreover, our data also shows that expression of *GCDH*, from the PGK promoter provides with a GCDH activity that is sufficient to prevent from the damage effects induced by the accumulation of GA or 3-OHGA in neurons. Consequently, *GCDH* gene replacement can be envisioned as a potential gene therapy strategy for GA1 patients.

DATA AVAILABILITY. Data is available within the published article and supplementary files. Additional data are available from corresponding author on reasonable request.

REFERENCES

1. Goodman SI, Markey SP, Moe PG, Miles BS, Teng CC. Glutaric aciduria; a “new” disorder of amino acid metabolism. Biochem Med. 1975 Jan;12(1):12–21.
2. Schuurmans IME, Dimitrov B, Schröter J, Ribes A, de la Fuente RP, Zamora B, et al. Exploring genotype–phenotype correlations in glutaric aciduria type 1. J Inherit Metab Dis. 2023;46(3):371–90.
3. Yuan Y, Dimitrov B, Boy N, Gleich F, Zielonka M, Kölker S. Phenotypic prediction in glutaric aciduria type 1 combining in silico and in vitro modeling with real-world data. J Inherit Metab Dis. 2023;46(3):391–405.
4. Kölker S, Sauer SW, Hoffmann GF, Müller I, Morath MA, Okun JG. Pathogenesis of

CNS involvement in disorders of amino and organic acid metabolism. J Inherit Metab Dis. 2008 Apr;31(2):194–204.

5. Kölker S, Garbade SF, Greenberg CR, Leonard J V., Saudubray JM, Ribes A, et al. Natural history, outcome, and treatment efficacy in children and adults with glutaryl-CoA dehydrogenase deficiency. Pediatr Res. 2006;59(6):840–7.

6. Pérez-Dueñas B, De La Osa A, Capdevila A, Navarro-Sastre A, Leist A, Ribes A, et al. Brain injury in glutaric aciduria type I: the value of functional techniques in magnetic resonance imaging. Eur J Paediatr Neurol EJPN Off J Eur Paediatr Neurol Soc. 2009 Nov;13(6):534–40.

7. Couce ML, López-Suárez O, Bóveda MD, Castiñeiras DE, Cocho JA, García-Villoria J, et al. Glutaric aciduria type I: outcome of patients with early- versus late-diagnosis. Eur J Paediatr Neurol EJPN Off J Eur Paediatr Neurol Soc. 2013 Jul;17(4):383–9.

8. Boy N, Mühlhausen C, Maier EM, Heringer J, Assmann B, Burgard P, et al. Proposed recommendations for diagnosing and managing individuals with glutaric aciduria type I: second revision. J Inherit Metab Dis. 2017 Jan;40(1):75–101.

9. Boy N, Mühlhausen C, Maier EM, Ballhausen D, Baumgartner MR, Beblo S, et al. Recommendations for diagnosing and managing individuals with glutaric aciduria type 1: third revision. J Inherit Metab Dis. 2022;

10. Busquets C, Begon˜ B, Merinero B, Julia´ J, Vaquerizo J, Orozco M, et al. Glutaryl-CoA Dehydrogenase Deficiency in Spain: Evidence of Two Groups of Patients, Genetically, and Biochemically Distinct. 2000.

11. Koeller DM, Woontner M, Crnic LS, Kleinschmidt-DeMasters B, Stephens J, Hunt EL, et al. Biochemical, pathologic and behavioral analysis of a mouse model of glutaric acidemia type I. Hum Mol Genet. 2002 Feb;11(4):347–57.

12. Zinnanti WJ, Lazovic J, Housman C, LaNoue K, O'Callaghan JP, Simpson I, et al. Mechanism of age-dependent susceptibility and novel treatment strategy in glutaric

acidemia type I. J Clin Invest. 2007 Nov;117(11):3258–70.

13. Zinnanti WJ, Lazovic J, Wolpert EB, Antonetti DA, Smith MB, Connor JR, et al. A diet-induced mouse model for glutaric aciduria type I. Brain. 2006 Apr;129(Pt 4):899–910.

14. Sauer SW, Okun JG, Fricker G, Mahringer A, Müller I, Crnic LR, et al. Intracerebral accumulation of glutaric and 3-hydroxyglutaric acids secondary to limited flux across the blood-brain barrier constitute a biochemical risk factor for neurodegeneration in glutaryl-CoA dehydrogenase deficiency. J Neurochem. 2006;97(3):899–910.

15. Kölker S, Koeller DM, Okun JG, Hoffmann GF. Pathomechanisms of neurodegeneration in glutaryl-CoA dehydrogenase deficiency. Ann Neurol. 2004 Jan;55(1):7–12.

16. Rodrigues MDN, Seminotti B, Amaral AU, Leipnitz G, Goodman SI, Woontner M, et al. Experimental evidence that overexpression of NR2B glutamate receptor subunit is associated with brain vacuolation in adult glutaryl-CoA dehydrogenase deficient mice: A potential role for glutamatergic-induced excitotoxicity in GA I neuropathology. J Neurol Sci. 2015 Dec;359(1–2):133–40.

17. Rio P, Baños R, Lombardo A, Quintana-Bustamante O, Alvarez L, Garate Z, et al. Targeted gene therapy and cell reprogramming in Fanconi anemia. EMBO Mol Med. 2014 Jun;6(6):835–48.

18. Shipley MM, Mangold CA, Szpara ML. Differentiation of the SH-SY5Y Human Neuroblastoma Cell Line. J Vis Exp. 2016 Feb;(108):53193.

19. Wittig I, Braun H-P, Schägger H. Blue native PAGE. Nat Protoc. 2006;1(1):418–28.

20. Janero DR. Malondialdehyde and thiobarbituric acid-reactivity as diagnostic indices of lipid peroxidation and peroxidative tissue injury. Free Radic Biol Med. 1990;9(6):515–40.

21. Baric I, Wagner L, Feyh P, Liesert M, Buckel W, Hoffmann GF. Sensitivity and specificity of free and total glutaric acid and 3-hydroxyglutaric acid measurements by

stable-isotope dilution assays for the diagnosis of glutaric aciduria type I. J Inherit Metab Dis. 1999 Dec;22(8):867–81.

22. Cudré-Cung HP, Remacle N, do Vale-Pereira S, Gonzalez M, Henry H, Ivanisevic J, et al. Ammonium accumulation and chemokine decrease in culture media of Gcdh−/− 3D reaggregated brain cell cultures. Mol Genet Metab [Internet]. 2019;126(4):416–28. Available from: https://doi.org/10.1016/j.ymgme.2019.01.009

23. Gao J, Zhang C, Fu X, Yi Q, Tian F, Ning Q, et al. Effects of Targeted Suppression of Glutaryl-CoA Dehydrogenase by Lentivirus-Mediated shRNA and Excessive Intake of Lysine on Apoptosis in Rat Striatal Neurons. PLoS One. 2013 May 2;8(5).

24. Fu X, Gao H, Tian F, Gao J, Lou L, Liang Y, et al. Mechanistic effects of amino acids and glucose in a novel glutaric aciduria type 1 cell model. PLoS One. 2014;9(10):e110181.

25. Olivera-Bravo S, Ribeiro CAJ, Isasi E, Trías E, Leipnitz G, Díaz-Amarilla P, et al. Striatal neuronal death mediated by astrocytes from the Gcdh-/- mouse model of glutaric acidemia type I. Hum Mol Genet. 2015 Aug;24(16):4504–15.

26. Schauwecker PE, Steward O. Genetic determinants of susceptibility to excitotoxic cell death: implications for gene targeting approaches. Proc Natl Acad Sci U S A. 1997 Apr;94(8):4103–8.

27. Martin LJ, Chang Q. DNA damage response and repair, DNA methylation, and cell death in human neurons and experimental animal neurons are different. J Neuropathol Exp Neurol. 2018;77(7):636–55.

28. Li J, Pan L, Pembroke WG, Rexach JE, Godoy MI, Condro MC, et al. Conservation and divergence of vulnerability and responses to stressors between human and mouse astrocytes. Nat Commun. 2021 Jun;12(1):3958.

29. Bakken TE, van Velthoven CT, Menon V, Hodge RD, Yao Z, Nguyen TN, et al. Single-cell and single-nucleus RNA-seq uncovers shared and distinct axes of variation in

dorsal LGN neurons in mice, non-human primates, and humans. Elife. 2021 Sep;10.

30. Loor G, Kondapalli J, Schriewer JM, Chandel NS, Vanden Hoek TL, Schumacker PT. Menadione triggers cell death through ROS-dependent mechanisms involving PARP activation without requiring apoptosis. Free Radic Biol Med. 2010 Dec;49(12):1925–36.

31. Rodrigues MDN, Seminotti B, Zanatta Â, de Mello Gonçalves A, Bellaver B, Amaral AU, et al. Higher Vulnerability of Menadione-Exposed Cortical Astrocytes of Glutaryl-CoA Dehydrogenase Deficient Mice to Oxidative Stress, Mitochondrial Dysfunction, and Cell Death: Implications for the Neurodegeneration in Glutaric Aciduria Type I. Mol Neurobiol. 2017 Aug;54(6):4795–805.

32. Tripathi R, Gupta R, Sahu M, Srivastava D, Das A, Ambasta RK, et al. Free radical biology in neurological manifestations: mechanisms to therapeutics interventions. Environ Sci Pollut Res Int. 2022 Sep;29(41):62160–207.

33. Seminotti B, Amaral AU, da Rosa MS, Fernandes CG, Leipnitz G, Olivera-Bravo S, et al. Disruption of brain redox homeostasis in glutaryl-CoA dehydrogenase deficient mice treated with high dietary lysine supplementation. Mol Genet Metab. 2013 Jan;108(1):30–9.

ACKNOWLEDGEMENTS

We thank Paula del Río for providing us with the plasmid pCCL.PGK.FANCA.WPRE. We are indebted to the Flow Cytometry Platform of IDIBAPS for technical help.

AUTHOR CONTRIBUTIONS

AM-B and ES-B performed the functional experiments and prepared the figures. JG-V developed the methods for metabolite analysis helped on the metabolite analysis, SG-S generated the constructs and contributed with some functional experiments. FT participated in the GCDH enzyme activity assays, GG and MG-M helped with the analysis of lipid peroxidation, AR provided GA1 pathology expertise and contributed to manuscript writing, JC, IR and JR performed the FISH analysis, CF coordinated the study and wrote the manuscript.

FUNDING

AM-B is recipient of a PIF-Salut predoctoral contract from Generalitat de Catalunya, Spain. MG-M is recipient of a Sara Borrell contract CD21/00019 from Instituto de Salud Carlos III (ISCIII). This work was supported by grants to CF from the CIVP19A5949-Fundación Ramon Areces, Merck Sharp Dohme España S.A, ACCI-CIBERER (ER21P2AC737) and PID2020-119692RB-C22 Spanish Ministerio de Ciencia e Innovación, with partial support from the Generalitat de Catalunya SGR2021/01169 and SGR2021/01423. It also acknowledges the support of CHARLIE Consortium, a project supported by ISCIII under the frame of E-Rare-3, the ERA-Net for Research on Rare Diseases, EJPRD grant nr: 825575. CIBERER is an initiative of the ISCIII. We also acknowledge the support of CERCA Programme/Generalitat de Catalunya. This work was developed at the Centro Esther Koplowitz, Barcelona, Spain.

ETHICAL APPROVAL

The authors declare compliance with ethical standards

COMPETING INTERESTS. The authors declare no competing financial interests.

FIGURE LEGENDS

Fig. 1. Characterization of SH-SY5Y *GCDH*-KO and SH-SY5Y *GCDH*-GI cells. A) Western blot showing *GCDH*-KO and GCDH expression in WT and *GCDH*-GI cells. B) In gel enzymatic GCDH activity in WT and GCDH-GI cells. C) Metabolite quantification: Glutarylcarnitine (C5DC), glutaric acid (GA) and 3-hydroxyglutaric acid (3-OHGA) were measured in the media of SH-SY5Y- WT, SH-SY5Y *GCDH*-KO and SH-SY5Y *GCDH*-GI after 48h of 10mM Lys exposure (n=4-6). Data shown as mean ± SEM; Mann-Whitney test: *p<0.05, ** p<0.01.

Fig. 2. Glutaric acid triggers SH-SY5Y *GCDH*-KO cell death (A) Cells were exposed to Glutaric acid (0-10-50-100 mM) and MTT assays were performed 24h later (n=8-9). B) qPCR mRNA quantification of caspase 3 levels in cells exposed to 50mM of GA for 6h (n=6-8). Data shown as mean ± SEM; Mann-Whitney test: *p < 0.05, **p < 0.01.

Fig. 3. Lysine exposure compromises neuronal SH-SY5Y *GCDH*-KO metabolic activity. Cells were exposed to Lys (0-10-25 mM) for 24h. (A) MTT assays (n=8-9) (B) Hoechst 33342 fluorescence quantification (n=4). Results are expressed as Relative Fluorescent Units (RFU). (C) Annexin V-FITC/PI apoptotic cells quantification (n=4). Data shown as mean ± SEM; Mann-Whitney test: *p < 0.05, **p < 0.01, ***p < 0.001.

Fig. 4. SH-SY5Y *GCDH*-KO cells are susceptible to oxidative stress. Cells were exposed to 10mM Lys for 72h. (A) Mitochondrial superoxide anion levels were analyzed by MitoSOXRed staining (n=3). (B) Antioxidant capacity was measured by SOD2 ELISA assay (n=4). (C) TBARS lipid peroxidation assay. MDA levels were measured (n=5). Data shown as mean ± SEM; Mann-Whitney test: *p < 0.05.

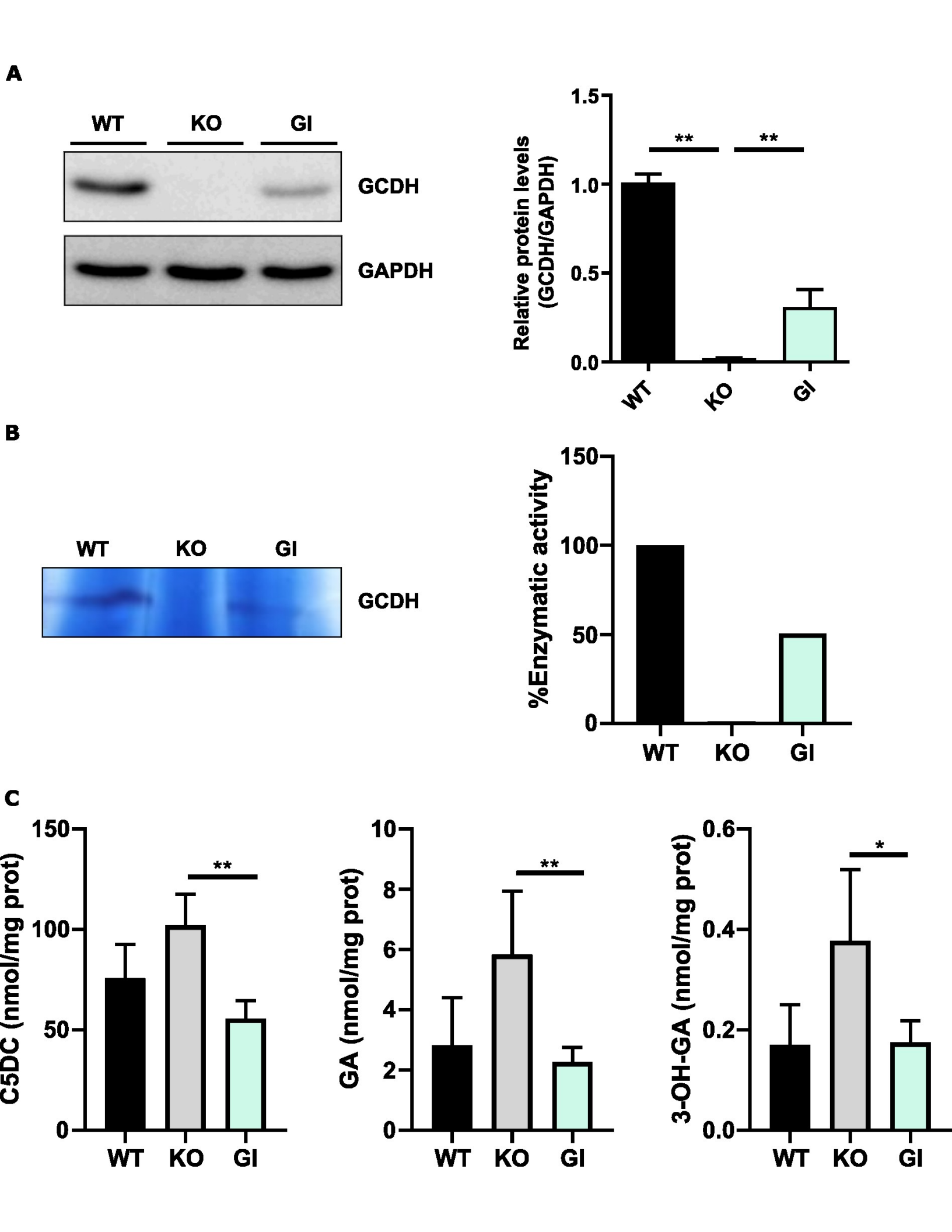
A
WT
KO
GI
GCDH
GAPDH
Relative protein levels (GCDH/GAPDH)
1.5
1.0
0.5
0.0
**
**
WT
KO
GI
B
WT
KO
GI
GCDH
%Enzymatic activity
150
100
50
0
WT
KO
GI
C
C5DC (nmol/mg prot)
150
100
50
0
**
WT
KO
GI
GA (nmol/mg prot)
10
8
6
4
2
0
**
WT
KO
GI
3-OH-GA (nmol/mg prot)
0.6
0.4
0.2
0.0
*
WT
KO
GI

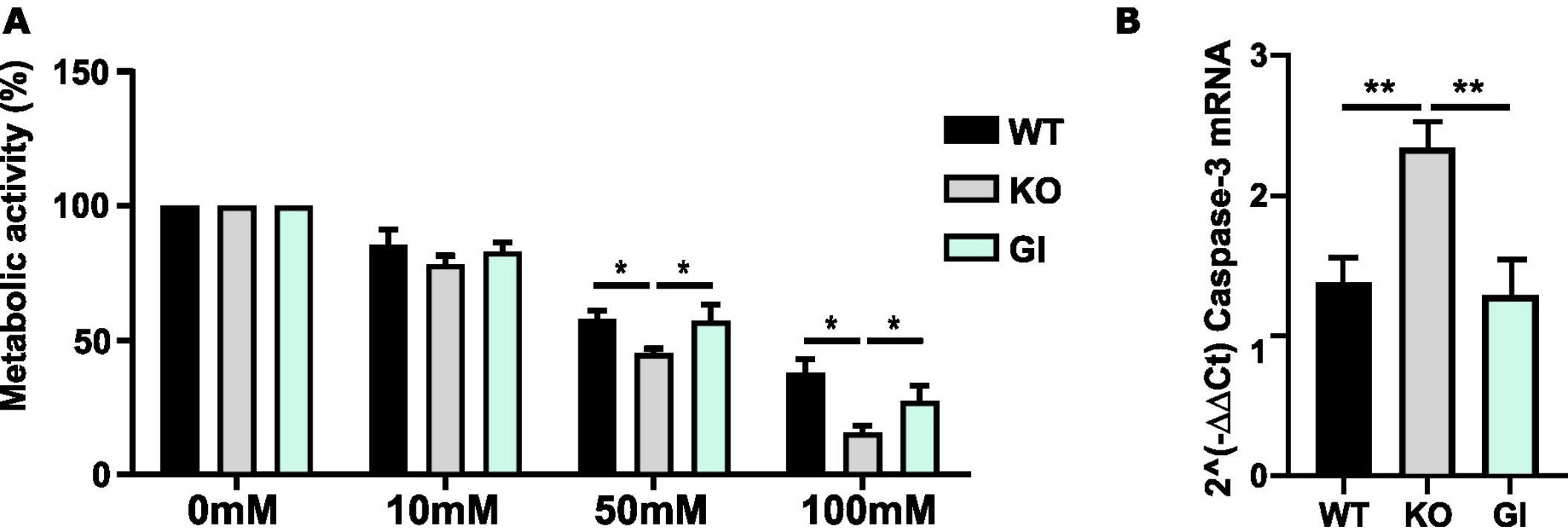
A
Metabolic activity (%)
150
100
50
0
0mM
10mM
50mM
100mM
WT
KO
GI
*
*
*
*
B
2^(-ΔΔCt) Caspase-3 mRNA
3
2
1
0
**
**
WT
KO
GI

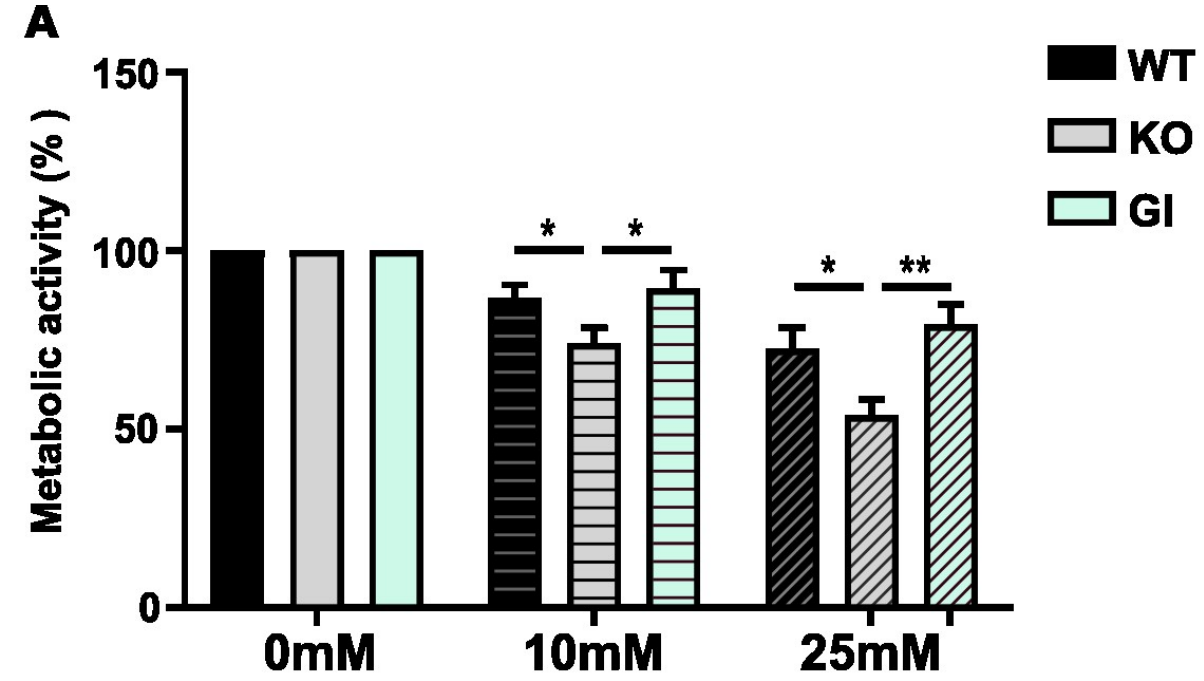
A
Metabolic activity (%)
150
100
50
0
0mM
10mM
25mM
WT
KO
GI
*
*
*
**

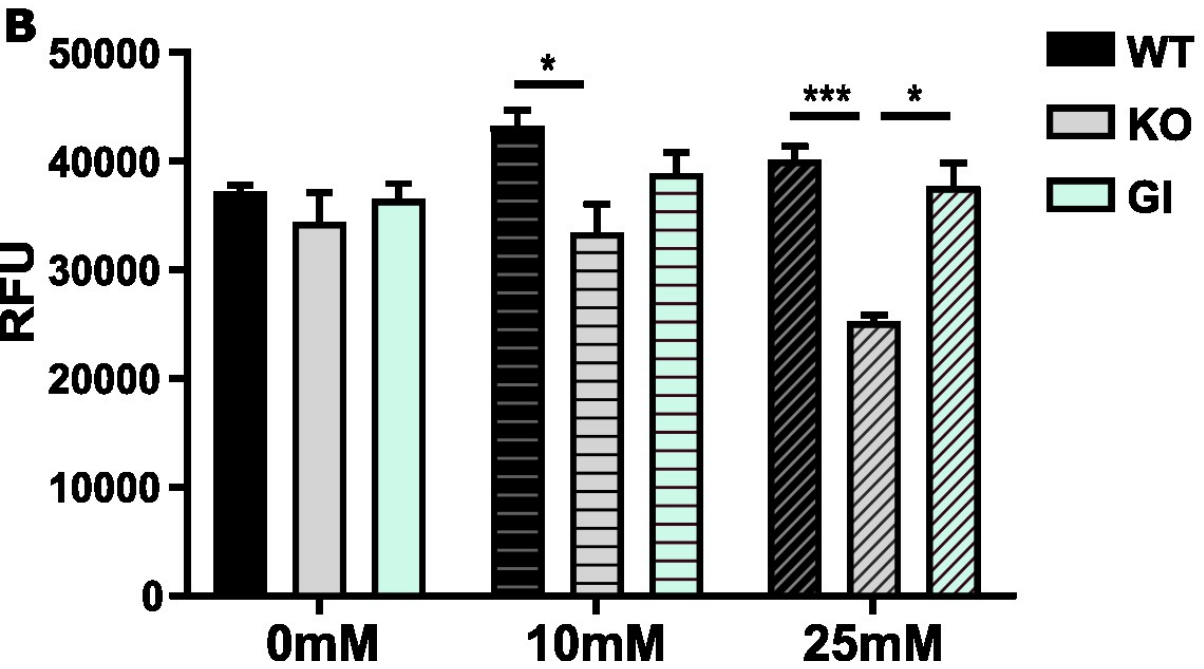
B
RFU
50000
40000
30000
20000
10000
0
0mM
10mM
25mM
WT
KO
GI
*
***
*

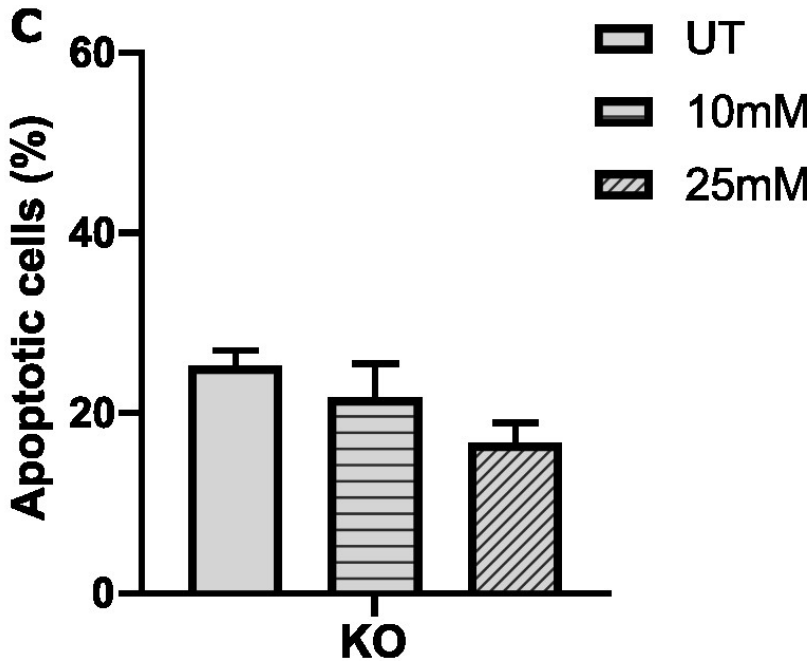
C
Apoptotic cells (%)
60
40
20
0
KO
UT
10mM
25mM

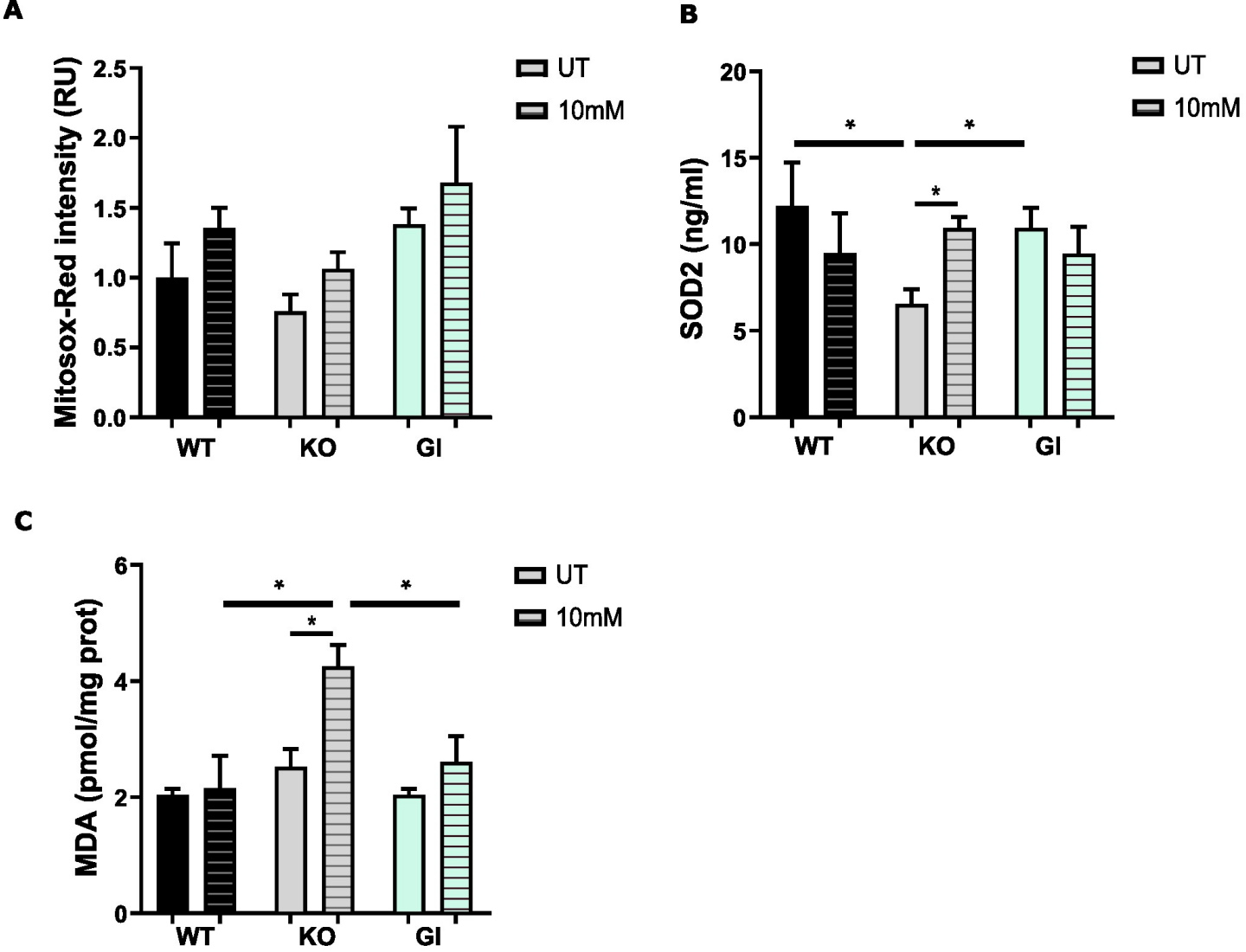
A
Mitosox-Red intensity (RU)
2.5
2.0
1.5
1.0
0.5
0.0
WT
KO
GI
UT
10mM
B
SOD2 (ng/ml)
20
15
10
5
0
*
*
*
WT
KO
GI
UT
10mM
C
MDA (pmol/mg prot)
6
4
2
0
*
*
*
WT
KO
GI
UT
10mM

Supplementary Figures

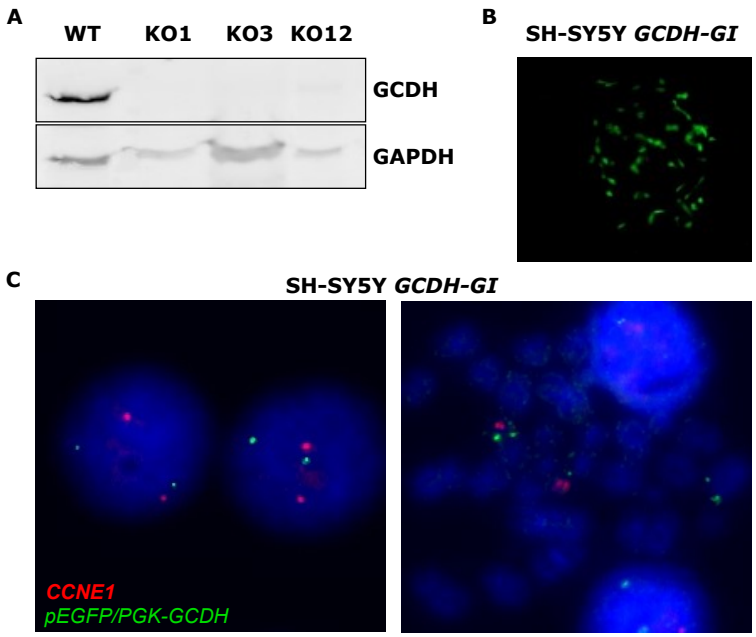

Supplementary Fig. 1. Generation of SH-SY5Y *GCDH*-KO and SH-SY5Y *GCDH*-GI cell lines. A) Western blot showing GCDH expression in WT and the lack of expression in KO clones. B) Representative image of GI cells expressing EGFP indicating integration of the construct. C): Interphase FISH analysis (left panel) showed two signals in the majority of the nuceli. Analysis of metaphases (right panel) indicated the localization of one copy of the construct at chromosome 19p (colocalization with *CCNE1* in the same chromosome) while the other copy of the construct was inserted in a different chromosome.

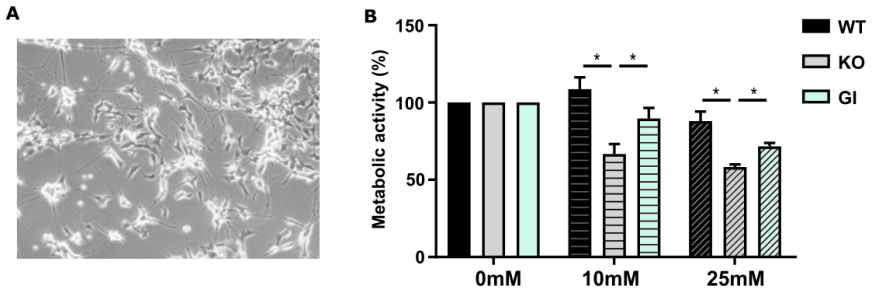

Supplementary Fig. 2. Susceptibility of differentiated neurons to Lysine overload. (A) Representative image of SH-SY5Y *GCDH*-KO differentiated cells. (B) SH-SY5Y *GCDH*-KO, SH-SY5Y *GCDH*-WT and SH-SY5Y *GCDH*-GI differentiated cells were exposed to Lys (0-10-25 mM) and MTT assays were performed 24h later (n=4). Data shown as mean ± SEM; Mann-Whitney test: *p < 0.05.

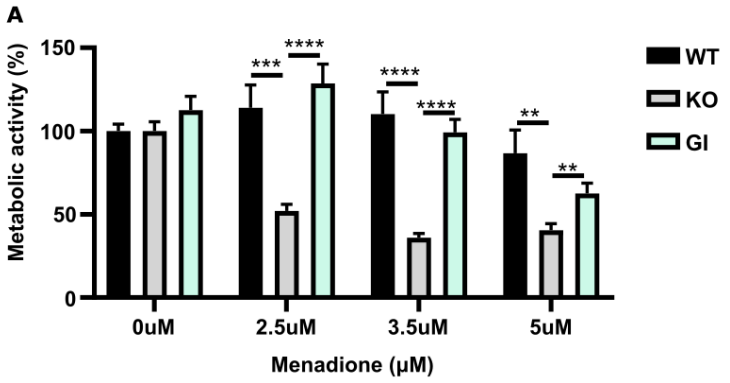

Supplementary Fig. 3. Susceptibility of of SH-SY5Y *GCDH*-WT SH-SY5Y *GCDH*-KO and SH-SY5Y *GCDH*-GI cells to Menadione treatment. (A) Cells were exposed to menadione at the indicated doses and MTT assays were performed 6h later (n=9). Data

shown as mean ± SEM; Mann-Whitney test: *p < 0.05, **p < 0.01, ***p < 0.001, ****p < 0.0001.

Supplementary Materials and Methods

FISH analysis

Metaphase harvesting was performed according to standard protocols through treatment with Colcemid, hypotonic solution and fixed with methanol:acetic acid (3:1). FISH was performed using SpectrumRed and SpectrumGreen-conjugated DNA BAC probes for *CCDE1* (CTD-3087O4) and the pEGFP/PGK-*GCDH* construct, respectively. Hybridization, washes, and detection was performed according to standard procedures. Slides were counterstained with DAPI and examined under a Nikon Eclipse 90i fluorescence microscope (Melville, NY, USA).

MTT Assay

A total of $5 \cdot 10^4$ cells of SH-SY5Y WT (wild type), *GCDH*-KO (Knockout) and *GCDH*-GI (GCDH Inserted) were seeded in triplicate into a 96 well plate and incubated with medium containing 0-10-25 mM lysine (SIGMA, St. Louis, MO, USA) or 0-10-50-100 mM of Glutaric acid (SIGMA) for 24h. Metabolic activity was measured using the MTT colorimetric assay (USB, Affymetrix, Santa Clara, CA USA).

Western Blot

Total protein extracts were obtained with lysis buffer (50 mM Tris-HCl (pH6.8), 2% SDS and 10% Glycerol) containing Complete Mini Protease Inhibitor Cocktail (Roche Diagnostics, Basel, Switzerland). Cell lysates were boiled for 10 min at 98°C. Protein concentration was

determined by BCA Protein Assay Kit (Thermo Fisher Scientific, Waltham, MA, USA) and 80 µg of total protein was resolved in 10% SDS-PAGE and transferred to nitrocellulose membrane. Membranes were immunoblotted with anti-GCDH polyclonal antibody (1:1000, overnight at 4°C, Sigma-Aldrich, #HPA043252), or anti-GAPDH (1/3000, 1 h at room temperature, Millipore, #ABS16, Burlington, VT, USA), rinsed with TBS-Tween. The secondary fluorescent antibody used was the IRDye 800CW Donkey anti-Rabbit IgG (LI-COR Biosciences, Lincoln, Nebraska, USA) (1/20000, 1h at room temperature). Fluorescent signal was acquired by the Odyssey Imaging System (LI-COR Biosciences, Lincoln, Nebraska,USA).

Antioxidant response analysis

SOD2 quantification was measured in cell extracts by Human SOD2 ELISA Kit (E-EL-H6188, Elabscience, Houston, TX, USA) in duplicates using an internal standard curve.